Journal of Modern Optics
Vol. 56, No. 6, 20 March 2009, 716–721

Highly efficient four-wave mixing via intersubband transitions in InGaAs/AlAs coupled double quantum well structures

Wen-Xing Yang[a,b]*, Jing-Min Hou[a] and Ray-Kuang Lee[b]

[a]*Department of Physics, Southeast University, Nanjing, China;* [b]*Institute of Photonics Technologies, National Tsing-Hua University, Hsinchu, Taiwan*

(*Received 31 March 2008; final version received 22 April 2008*)

We perform a time-dependent analysis of continuous wave (cw) four-wave mixing (FWM) in InGaAs/AlAs coupled double quantum well (CDQW) structures via intersubband transitions. By using the coupled Schrödinger–Maxwell approach, we obtain the corresponding explicit analytical expressions for the input probe and FWM-generated signal fields. We calculated the dependencies of the efficiency of the FWM-generated fields on cw pump fields and the depths of penetration into the CDQW sample. Such a nonlinear optical process may be used to generate coherent short-wavelength radiation efficiently in the CDQW solid state system.

Keywords: four-wave mixing; quantum well; quantum coherence

The effects of quantum coherence and interference in quantum and nonlinear optical phenomena in highly resonant media have attracted significant interest in the past decade due to interesting applications in nonlinear optics. One of the interesting phenomena is the multiwave mixing process. For example, Harris et al. proposed a FWM scheme and showed that the FWM efficiency could be greatly enhanced [1]; Zibrov et al. investigated an efficient nonlinear process in a four-level resonant atomic media with counter-propagating fields and showed that such a process can be used for generation of pairs of Stokes and anti-Stokes fields [2]. Recently, Deng et al. studied the optical coherent FWM with a weak probe wave based on electromagnetically induced transparency (EIT) and showed that such a scheme could lead to many orders of magnitude enhancement in the amplitude of the generated wave in a typical four-level atomic system [3]. Later, Wu et al. analyzed and discussed a FWM scheme in a five-level atomic system and hyper-Raman scattering (HRS) in resonant coherent media by the use of EIT, which led to the suppression of both single-photon, two-photon and three-photon absorptions in both FWM and HRS schemes and enabling the four-wave mixing to proceed through real, resonant intermediate states without absorption loss [4,5]. Consequently, a robust three-photon destructive interference between the two different excitation channels occurs, resulting in a saturated FWM production [6,7]. In addition, Kang et al. reported an experimental study of resonant six-wave mixing in coherently prepared four-level double-Λ Rb atomic media and they also reported an experimental observation of resonantly enhanced slow-light four-wave mixing in such cold Rb atomic media, which may open up new opportunities for technological applications of these predicted phenomena [8].

It is easy to implement quantum coherence and interference in optically dense atomic samples in the gas phase, but it is more difficult to observe them in solid-state media because of short coherence times in solids. However, it is more advantageous at least from the view point of practical purposes [9]. Over the past few years, the similar phenomena involving EIT and ultraslow propagation of optical pulses via intersubband transitions (ISBT) in semiconductor quantum well systems have also attracted great attention due to the potentially important applications in optoelectronics and solid-state quantum information science [10–35]. In fact, the analogies between coherent nonlinear phenomena in atomic system and semiconductor models have been successfully exploited. For example, coherently controlled photocurrent generation [21], EIT [24], and gain without inversion [15–17], multiwave mixing [32], have been extensively investigated in semiconductor quantum well systems. In particular, quantum tunneling to a continuum from two resonant subband levels in asymmetric double quantum wells may give rise to Fano-type interference [12,13]; several authors have studied all optical switching based Fano interference in quantum wells [27,34]. In contrast, devices based on the intersubband transitions in the

*Corresponding author. Email: wenxingyang2@126.com

ISSN 0950–0340 print/ISSN 1362–3044 online

DOI: 10.1080/09500340802155404
http://www.informaworld.com

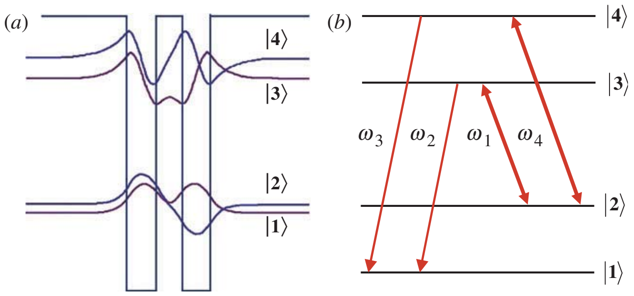

Figure 1. (*a*) A schematic diagram of a CDQW structure with two 2.3 nm wells separated by a 1.4 nm barrier, the purple lines for the symmetric states marked $|1\rangle$, $|3\rangle$ and the blue lines for the anti-symmetric ones marked $|2\rangle$, $|4\rangle$. (*b*) A schematic diagram of the energy level arrangement for the CDQW structure under study, the arrows indicate the allowed transitions of the $|1\rangle \leftrightarrow |3\rangle$, $|1\rangle \leftrightarrow |4\rangle$, $|2\rangle \leftrightarrow |3\rangle$, and $|2\rangle \leftrightarrow |4\rangle$. (The color version of this figure is included in the online version of the journal.)

semiconductor quantum wells have many inherent advantages in quantum information processing, such as large electric dipole moments due to the small effective electron mass, high nonlinear optical coefficients, and a great flexibility in device design by choosing the materials and structure dimensions. Furthermore, the transition energies, dipoles, and symmetries can be controlled at will.

In this paper, we demonstrate the efficient generation of coherent light in an asymmetric semiconductor double quantum well by using ISBT as shown in Figure 1, where a four-level coupled double quantum well (CDQW) interacts with two continuous pump fields (1) and (4) and a weak-pulsed field (2), and a pulsed FWM field (3) can then be generated efficiently. In the following analysis we assume that the CDQW structure with low doping are designed such that electron–electron effects have very small influence, as a result, many body effects arising from electron–electron interactions are not considered. Besides, we assume that all subbands have the same effective mass and the cw pump fields are strong enough.

The CDQW sample considered here could be very similar to the one reported in [36], where we can choose the proper parametric conditions. As a rule, the sample contains 100 coupled quantum wells and each coupled quantum well consists of 10 and 7 mono-layer (ML) $In_{0.5}Ga_{0.5}As$ quantum wells separated by a 3 ML thick AlAs layer as shown in Figure 1. The sample can be designed to have desired transition energies, i.e. E_{13} in the range of 128 meV, E_{14} in the range of 182 meV, E_{23} in the range of 142 meV, and E_{24} in the range of 168 meV. By adopting the standard approach [37], under the rotating-wave and electro-dipole approximations the interaction of the structure with fields can be described by the Schrödinger equation in the interaction picture,

$$i\hbar \frac{\partial |\psi\rangle}{\partial t} = H|\psi\rangle, \tag{1}$$

where the Hamiltonian ($H = H_0 + H_I$) reads

$$\frac{H_0}{\hbar} = \begin{pmatrix} 0 & 0 & 0 & 0 \\ 0 & -\Delta\omega_1 & 0 & 0 \\ 0 & 0 & -\Delta\omega_2 & 0 \\ 0 & 0 & 0 & -\Delta\omega_3 \end{pmatrix}, \tag{2}$$

$$\frac{H_I}{\hbar} = \begin{pmatrix} 0 & 0 & \Omega_2^* \exp(-ik_2 \cdot r) & \Omega_3^* \exp(-ik_3 \cdot r) \\ 0 & 0 & \Omega_1^* \exp(-ik_1 \cdot r) & \Omega_4^* \exp(-ik_4 \cdot r) \\ \Omega_2 \exp(ik_2 \cdot r) & \Omega_1 \exp(ik_1 \cdot r) & 0 & 0 \\ \Omega_3 \exp(ik_3 \cdot r) & \Omega_4 \exp(ik_4 \cdot r) & 0 & 0 \end{pmatrix}, \tag{3}$$

where $\Delta\omega_2 = \omega_2 - \epsilon_3/\hbar$, $\Delta\omega_1 = \omega_2 - \omega_1 - \epsilon_2/\hbar$, and $\Delta\omega_3 = \omega_2 - \omega_1 + \omega_4 - \epsilon_4/\hbar$ are the single-photon, two-photon, and three-photon detunings, respectively, and ϵ_j is the energy of the subband-level $|j\rangle$ ($j = 2, 3, 4$, taking $\epsilon_1 \equiv 0$ for the ground state), and $2\Omega_{1,2,3,4}$ are the Rabi frequencies of the relevant fields, i.e. $\Omega_2 = \mu_{31}E_2/(2\hbar)$, $\Omega_1 = \mu_{32}E_1/(2\hbar)$, $\Omega_4 = \mu_{42}E_4/(2\hbar)$, and $\Omega_3 = \mu_{41}E_3/(2\hbar)$ with μ_{ij} being the dipole moment between subbands $|i\rangle$ and $|j\rangle$, the k_j is the wave vector.

Let us assume the electronic wave function of the form

$$\left|\psi\right\rangle = (A_1, A_2 \exp[\mathrm{i}(k_2 - k_1)\cdot r], A_3 \exp(\mathrm{i}k_2 \cdot r), \times A_4 \exp[\mathrm{i}(k_2 - k_1 + k_4)\cdot r])^{\mathrm{T}}, \tag{4}$$

where $A_i (i = 1, 2, 3, 4)$ are the time-dependent probability amplitudes of finding the electron in subbands $|i\rangle$, and T present transpose. The equations of the motion for the probability amplitude of the electronic wave functions can be readily obtained as

$$\frac{\partial A_2}{\partial t} = -\mathrm{i}\Omega_4^* A_4 - \mathrm{i}\Omega_1^* A_3 + (\mathrm{i}\Delta\omega_1 + \gamma_2)A_2, \tag{5}$$

$$\frac{\partial A_3}{\partial t} = -\mathrm{i}\Omega_1 A_2 - \mathrm{i}\Omega_2 A_1 + (\mathrm{i}\Delta\omega_2 + \gamma_3)A_3, \tag{6}$$

$$\frac{\partial A_4}{\partial t} = -\mathrm{i}\Omega_3 \exp(\delta k \cdot r)A_1 - \mathrm{i}\Omega_4 A_2 + (\mathrm{i}\Delta\omega_3 + \gamma_4)A_4, \tag{7}$$

where γ_j $(j = 2, 3, 4)$ is the total decay rate of the subbands $|j\rangle$, which is added phenomenologically in the above coupled amplitude equations. Also, we have introduced the k-wavevector mismatched condition $\delta k = k_3 - k_2 + k_1 - k_4$. It should be noted that, in semiconductor quantum wells, the total decay rates γ_i of subbands $|i\rangle$ comprises a population-decay contribution γ_{il} as well as a dephasing contribution γ_{id}, i.e. $\gamma_i = \gamma_{il} + \gamma_{id}$. The former γ_{il} is due primarily to longitudinal optical (LO) photon emission events at low temperature. The latter γ_{id} may originate not only from electron–electron scattering and electron–phonon scattering, but also from inhomogeneous broadening due to scattering on interface roughness. The population decay rates can be calculated by solving the effective mass Schrödinger equation. And as we know, the initially nonthermal carrier distribution is quickly broadened due to inelastic carrier–carrier scattering, with the broadening rate increasing as carrier density is increased. For temperatures up to 10 K and the carrier density smaller than $6 \times 10^{11}\,\mathrm{cm}^{-2}$, the dephasing decay rates $\gamma_{ij}^{\mathrm{dph}}$ can be estimated according to [13,26].

We choose the two fields ω_2 and ω_1 to propagate in the same direction and so do the other two fields ω_3 and ω_4. More strictly speaking, the FWM generated field propagating in the opposite direction to field ω_2 does not satisfy the phase-matching condition and hence is much smaller than the FWM-generated field propagating in the same direction as the field ω_2. Then we can take $k_2 \approx k_1$ and $k_3 \approx k_4$, leading to $\delta k \approx 0$. In the limit of a weak probe signal ($\Omega_1 \gg \Omega_2$, $\Omega_4 \gg \Omega_3$), almost all electrons will remain in the subband level $|1\rangle$ due to the fact that the electron–field interaction is weak and hence we may assume that $A_1 \approx 1$. Under this assumption, we can then obtain straightforwardly the steady-state solutions of Equations (5)–(7) as follows:

$$A_2 = \frac{D_3\Omega_1^*\Omega_2 + D_2\Omega_4^*\Omega_3}{(D_3D_1 - |\Omega_4|^2)D_2 - D_3|\Omega_1|^2}, \tag{8}$$

$$A_3 = \frac{(D_3D_1 - |\Omega_4|^2)\Omega_2 + \Omega_1\Omega_4^*\Omega_3}{(D_3D_1 - |\Omega_4|^2)D_2 - D_3|\Omega_1|^2}, \tag{9}$$

$$A_4 = \frac{(D_2D_1 - |\Omega_1|^2)\Omega_3 + \Omega_1^*\Omega_4\Omega_2}{(D_3D_1 - |\Omega_4|^2)D_2 - D_3|\Omega_1|^2}, \tag{10}$$

where $D_1 = \Delta\omega_1 + \mathrm{i}\gamma_2$, $D_2 = \Delta\omega_2 + \mathrm{i}\gamma_3$, and $D_3 = \Delta\omega_3 + \mathrm{i}\gamma_4$. According to the polarizations of fields $P_j(z, t) = (1/2)\varepsilon_0 P_{js} \exp(\mathrm{i}k_j \cdot r - \mathrm{i}\omega_j t) + c.c.$ $(j = 2, 3)$, the slowly varying parts P_{js} of the polarization of the input probe field (2) and the FWM generated field (3) can be derived as

$$P_{js} = \frac{N\mu_{41}A_4A_1^*}{\varepsilon_0} = \frac{N\mu_{31}\mu_{41}\Omega_1^*\Omega_4}{2\hbar\varepsilon_0(D_3D_1 - |\Omega_4|^2)D_2 - D_3|\Omega_1|^2}E_2 + \chi(\omega_3)E_3, \tag{11}$$

$$P_{js} = \frac{N\mu_{31}A_3A_1^*}{\varepsilon_0} = \frac{N\mu_{31}\mu_{41}\Omega_1\Omega_4^*}{2\hbar\varepsilon_0(D_3D_1 - |\Omega_4|^2)D_2 - D_3|\Omega_1|^2}E_3 + \chi(\omega_2)E_2, \tag{12}$$

where N is the electron density in the conduction band of a quantum well. Here the linear susceptibilities are

$$\chi(\omega_3) = \frac{N|\mu_{41}|^2(D_2D_1 - |\Omega_1|^2)}{2\hbar\varepsilon_0(D_3D_1 - |\Omega_4|^2)D_2 - D_3|\Omega_1|^2}, \tag{13}$$

$$\chi(\omega_2) = \frac{N|\mu_{31}|^2(D_3D_1 - |\Omega_4|^2)}{2\hbar\varepsilon_0(D_3D_1 - |\Omega_4|^2)D_2 - D_3|\Omega_1|^2}. \tag{14}$$

As a result, under the slowly varying amplitude approximation, the input probe and generated FWM fields propagating along the 'z' direction evolve according to

$$\frac{\partial\Omega_3}{\partial z} = \mathrm{i}\frac{\omega_3}{2c}\left[\frac{N|\mu_{41}|^2\Omega_1^*\Omega_4\Omega_2}{2\hbar\varepsilon_0(D_3D_1 - |\Omega_4|^2)D_2 - D_3|\Omega_1|^2} + \frac{N|\mu_{41}|^2(D_2D_1 - |\Omega_1|^2)\Omega_3}{2\hbar\varepsilon_0(D_3D_1 - |\Omega_4|^2)D_2 - D_3|\Omega_1|^2}\right], \tag{15}$$

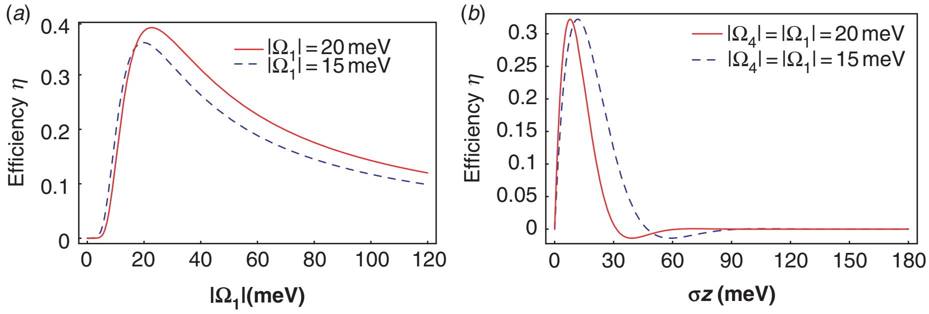

Figure 2. (*a*) Dependence of the FWM efficiency η on the cw pump field (4) strength $|\Omega_4|$ for another cw pump field strength $|\Omega_1| = 15$, 20 meV with $\sigma L = 30$ meV; (*b*) dependence of the FWM efficiency η on the depth z of penetration into the CDQW sample with $|\Omega_4| = |\Omega_1| = 15$, 20 meV. Other fitting parameters are $\Delta\omega_1 = \Delta\omega_2 = \Delta\omega_3 = 0$, $\gamma_3 = \gamma_4 = 8$ meV, $\gamma_2 = 5$ meV, and $\omega_3 = 1.25\omega_2$. (The color version of this figure is included in the online version of the journal.)

$$\frac{\partial\Omega_2}{\partial z} = \mathrm{i}\frac{\omega_2}{2c}\left[\frac{N|\mu_{31}|^2\Omega_1\Omega_4^*\Omega_3}{2\hbar\varepsilon_0(D_3D_1 - |\Omega_4|^2)D_2 - D_3|\Omega_1|^2} + \frac{N|\mu_{31}|^2(D_3D_1 - |\Omega_4|^2)\Omega_2}{2\hbar\varepsilon_0(D_3D_1 - |\Omega_4|^2)D_2 - D_3|\Omega_1|^2}\right]. \quad (16)$$

Equations (15) and (16) can be readily solved under the boundary conditions $\Omega_3(z=0) = 0$ and $\Omega_2(z=0) \neq 0$ with further assumption that pump fields $\Omega_{1,4}$ are the constants. The general solutions of Equations (15) and (16) are given by

$$\Omega_3(z) = \Omega_2(0)2\mathrm{i}\exp(\mathrm{i}GS_+)\left(\frac{\omega_3}{\omega_2}\right)^{1/2} \times \frac{\mu_{41}\Omega_1^*\Omega_4}{\mu_{31}|\Omega_1\Omega_4|}\frac{\sin\left((4+S_-^2)^{1/2}G\right)}{(4+S_-^2)^{1/2}}, \quad (17)$$

$$\Omega_2(z) = \Omega_2(0)\exp(\mathrm{i}GS_+) \times \left[\cos\left((4+S_-^2)^{1/2}G\right) + \mathrm{i}S_-\frac{\sin\left((4+S_-^2)^{1/2}G\right)}{(4+S_-^2)^{1/2}}\right], \quad (18)$$

with

$$G = \frac{N(\omega_2\omega_3)^{1/2}|\mu_{31}\mu_{41}\Omega_1\Omega_4|z}{8\hbar c\varepsilon_0\left[(D_3D_1 - |\Omega_4|^2)D_2 - D_3|\Omega_1|^2\right]}, \quad (19)$$

$$S_\pm = \left(\frac{\omega_3}{\omega_2}\right)^{1/2}\left|\frac{\mu_{41}\Omega_1}{\mu_{31}\Omega_4}\right|\left(\frac{D_2D_1 - |\Omega_1|^2}{|\Omega_1|^2}\right) \pm \left(\frac{\omega_2}{\omega_3}\right)^{1/2}\left|\frac{\mu_{31}\Omega_4}{\mu_{41}\Omega_1}\right|\left(\frac{D_3D_1 - |\Omega_4|^2}{|\Omega_4|^2}\right), \quad (20)$$

where Equations (17) and (18) are the main results of the present study. Based on the definition of [8], the efficiency of the generated FWM field can be derived, i.e. $\eta = |E_3^{(\mathrm{out})}/E_2^{(\mathrm{in})}|^2$, where $E_3^{(\mathrm{out})}$ is the electric field E_3 of the FWM-generated field at the exit $z = L$ and $E_2^{(\mathrm{in})}$ is the electric field of the probe field at the entrance $z = 0$. According to Equations (17–20), the efficiency has the form,

$$\eta \simeq \frac{\omega_3\sigma_1\sigma_2|\Omega_1|^2|\Omega_4|^2\exp(-2\,\mathrm{Im}\,[\chi(\omega_3)]L)}{\omega_2\left(\left|\sigma_1|\Omega_1|^2 - \sigma_2|\Omega_4|^2\right|^2 + 4\sigma_1\sigma_2|\Omega_1|^2|\Omega_4|^2\right)}, \quad (21)$$

with $\sigma_1 = 2N\omega_3|\mu_{14}|^2/\hbar c$ and $\sigma_2 = 2N\omega_2|\mu_{13}|^2/\hbar c$. Based on the result of Equation (21), the dependence of the efficiency of the generated FWM field on both the strengths of the cw pump fields (4), (1) and the depths of penetration into the CDQW sample. The related results are illustrated in Figure 2. Figure 2(*a*) shows that the efficiency versus the strength of the cw pump field (4) for two different strength values of another cw pump field (1). The result from the plot shows that even for the depths of penetration into the CDQW sample as $\sigma L = 30$ meV, with appropriate cw pump field strengths, the efficiency ($\eta > 40\%$) indeed can be achieved. In addition, the maximum efficiency η is achieved with the same strength of the cw pump fields, i.e. $|\Omega_1| = |\Omega_4|$. In Figure 2(*b*), the efficiency is plotted for different depths of penetration into the CDQW sample for different strengths of cw pump fields (1) and (4) with always the same value of the two cw pump fields ($|\Omega_1| = |\Omega_4|$). The result from the plot shows that even for $|\Omega_1| = |\Omega_4| \sim 15$ meV, the efficiency ($\eta > 30\%$) could be obtained with appropriate CDQW parameters (i.e. σz). Besides, Figure 2(*b*) also shows that the efficiency η reaches an invariable value and is independent of the depth of penetration into the CDQW sample. This interesting result is produced by the combination of a constructive interference (induced by coupling excitation) and a destructive interference (induced by back-coupling excitation). When the generated-FWM field is sufficiently strong, the back-coupling excitation produces the destructive interference pathway, leading to the suppression of the

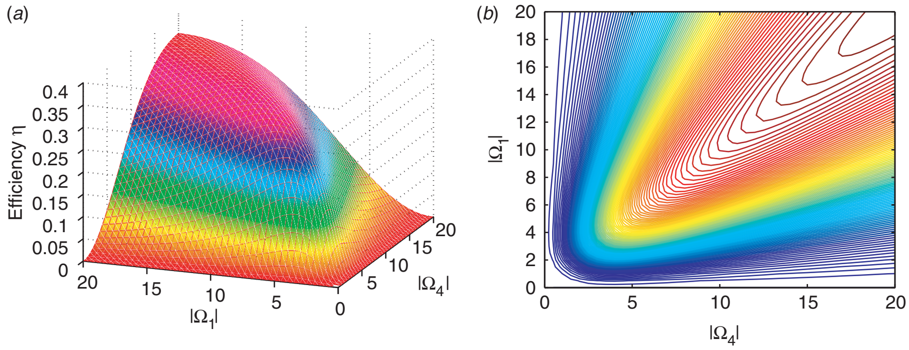

Figure 3. (*a*) Dependence of the FWM efficiency η on the two cw pump fields (1) and (4) strength $|\Omega_1|$ and $|\Omega_4|$ with $\sigma L = 30\,\text{meV}$. (*b*) The contour lines of (*a*). Other fitting parameters are $\Delta\omega_1 = \Delta\omega_2 = \Delta\omega_3 = 0$, $\gamma_3 = \gamma_4 = 8\,\text{meV}$, $\gamma_2 = 5\,\text{meV}$, and $\omega_3 = 1.25\omega_2$. (The color version of this figure is included in the online version of the journal.)

strength of FWM fields. The results of Figure 2(*a*) can be verified in Figures 3(*a*) and (*b*). Figure 3(*a*) shows the three-dimensional plot of the dependence of the FWM efficiency η on the strengths of two cw pump fields. The contour lines are shown in Figure 3(*b*), which indicates a locus of achieved maximum efficiency.

In summary, by using the coupled Schrödinger–Maxwell equations in a four-level system of electronic subbands, we have proposed and analyzed a novel scheme to achieve parametric generation of a new laser radiation with high conversion efficiency in CDQW structures based on ISBT, which is much more practical than that in an atomic system because of its flexible design and the controllable interference strength. We obtain the corresponding explicit analytical expressions for both the probe field and the FWM-generated field. Except for the inherent importance, our scheme may also open a new possibility for technological applications in the CDQW solid-state system.

Before ending, it is worth noting that we have used the one-dimensional model in analysis, and correspondingly, the momentum-dependency of subband energies was ignored. In fact, there is no large discrepancy between the reduced one-dimensional calculation and the full two-dimensional calculation, and the related theoretical discussions can be found in [23,24]. Besides, in order to obtain simple analytical expressions, we have adopted the Schrödinger formalism with adding decay rates phenomenally. There have been some works discussing theoretically the equivalence between the Schrödinger-formalism adding phenomenal decay rates with the density matrix formalism in dealing with the dephasing processes [6,9]. One can readily check by numerical computations that the results of our treatment are essentially the same as those from the usual density matrix formalism in the case that almost all the electrons remain in the subband level $|1\rangle$ (ground state).

Acknowledgements

The research is supported in part by National Natural Science Foundation of China under Grant Nos. 10704017, 10634060, 90503010 and 10575040, by National Fundamental Research Program of China 2005CB724508. WXY would like to acknowledge Xiangying Hao for her enlightening discussions.

References

[1] Harris, S.E.; Field, J.E.; Imamoglu, A. *Phys. Rev. Lett.* **1990,** *64,* 1107–1110.
[2] Zibrov, A.S.; Lukin, M.D.; Scully, M.O. *Phys. Rev. Lett.* **1999,** *83,* 4049–4052.
[3] Deng, L.; Kozuma, M.; Hagley, E.W.; Payne, M.G. *Phys. Rev. Lett.* **2002,** *88,* 143902-1–3.
[4] Wu, Y.; Saldana, J.; Zhu, Y. *Phys. Rev. A* **2003,** *67,* 013811-1–5.
[5] Wu, Y.; Wen, L.; Zhu, Y. *Opt. Lett.* **2003,** *28,* 631–633; Wu, Y.; Yang, X. *Phys. Rev. A* **2004,** *70,* 053818-1–5.
[6] Wu, Y.; Yang, X. *Phys. Rev. A* **2005,** *71,* 053806-1–7.
[7] Wu, Y.; Payne, M.G.; Hagley, E.W.; Deng, L. *Opt. Lett.* **2004,** *29,* 2294–2296; *Phys. Rev. A* **2004,** *70,* 063812-1–4.
[8] Kang, H.; Hernandez, G.; Zhu, Y. *Phys. Rev. Lett.* **2004,** *93,* 073601-1–4; *Phys. Rev. A* **2004,** *70,* 061804-1–4; Kang, H.; Hernandez, G.; Zhang, J.; Zhu, Y. *J. Opt. Soc. Am. B* **2006,** *23,* 718–723.
[9] Wu, Y.; Yang, X. Phys Rev. B *76,* **2007,** 054425-1–4; *Appl. Phys. Lett.* **2007,** *91,* 094104-1–3.
[10] Faist, J.; Sirtori, C.; Capasso, F.; Chu, S.N.G.; Pfeiffer, L.N.; West, K.W. *Opt. Lett.* **1996,** *21,* 985–987.
[11] Faist, J.; Capasso, F.; Sirtori, C.; West, K.; Pfeiffer, L.N. *Nature (London)* **1997,** *390,* 589–591.
[12] Faist, J.; Capasso, F.; Sirtori, C.; Sivco, D.L.; Hutchinson, A.L.; Chu, S.N.G.; Cho, A.Y. *Appl. Phys. Lett.* **1994,** *65,* 94–96; Faist, J.; Capasso, F.; Sirtori, C.;

Hutchinson, A.L.; West, K.W. *Appl. Phys. Lett.* **1997,** *71,* 3477–3479.
[13] Schmidt, H.; Campman, K.L.; Gossard, A.C.; Imamoglu, A. *Appl. Phys. Lett.* **1997,** *70,* 3455–3457; Phillips, M.; Wang, H. *Opt. Lett.* **2003,** *28,* 831–833; Ginzburg, P.; Orenstein, M. *Opt. Express* **2006,** *14,* 12467–12472.
[14] Schmidt, H.; Imamoglu, A. *Opt. Commun.* **1996,** *131,* 333–338.
[15] Imamoglu, A.; Ram, R.J. *Opt. Lett.* **1994,** *19,* 1744–1746; Nikonov, D.E.; Imamoglu, A.; Scully, M.O. *Phys. Rev. B* **1999,** *59,* 12212–12215.
[16] Lee, C.R.; Li, Y.C.; Men, F.K.; Pao, C.H.; Tsai, Y.C.; Wang, J.F. *Appl. Phys. Lett.* **2004,** *86,* 201112–201114.
[17] Frogley, M.D.; Dynes, J.F.; Beck, M.; Faist, J.; Phillips, C.C. *Nature Mater.* **2006,** *5,* 175–178.
[18] Gmachl, C. *Nature Mater.* **2006,** *5,* 169–170.
[19] Serapiglia, G.B.; Paspalakis, E.; Sirtori, C.; Vodopyanov, K.L.; Phillips, C.C. *Phys. Rev. Lett.* **2000,** *84,* 1019–1022.
[20] Li, T.; Wang, H.; Kwong, N.H.; Binder, R. *Opt. Express* **2003,** *11,* 3298–3303; Yang, X.X.; Li, Z.W.; Wu, Y. *Phys. Lett. A* **2005,** *340,* 320–325; Wu, Y.; Yang, X.X. *Opt. Lett.* **2005,** *30,* 311–313; Wu, Y.; Payne, M.G.; Hagley, E.W.; Deng, L. *Opt. Lett.* **2004,** *29,* 2294–2296.
[21] Atanasov, R.; Hache, A.; Hughes, J.L.P.; van Driel, H.M.; Sipe, J.E. *Phys. Rev. Lett.* **1996,** *76,* 1703–1706.
[22] Potz, W. *Physica E (Amsterdam)* **2000,** *7,* 159–167; *Phys. Rev. B* **2005,** *71,* 125331-1–14; Hu, X.; Potz, W. *Phys. Rev. Lett.* **1999,** *82,* 3116–3119; Muller, T.; Parz, W.; Strasser, G.; Unterrainer, K. *Phys. Rev. B* **2004,** *70,* 155324-1–5; *Appl. Phys. Lett.* **2004,** *84,* 64–66; Muller, T.; Bratschitsch, R.; Strasser, G.; Unterrainer, K. *Appl. Phys. Lett.* **2001,** *79,* 2755–2757.
[23] Waldmüller, I.; Förstner, J.; Lee, S.-C.; Knorr, A.; Woerner, M.; Reimann, K.; Kaindl, R.A.; Elsaesser, T.; Hey, R.; Ploog, K.H. *Phys. Rev. B* **2004,** *69,* 205307-1–9; Shih, T.; Reimann, K.; Woerner, M.; Elsaesser, T.; Waldmüller, I.; Knorr, A.; Hey, R.; Ploog, K.H. *Phys. Rev. B* **2005,** *72,* 195338-1–8; Richter, M.; Butscher, S.; Schaarschmidt, M.; Knorr, A. *Phys. Rev. B* **2007,** *75,* 115331-1–8; Butscher, S.; Knorr, A. *Phys. Rev. Lett.* **2006,** *97,* 197401-1–4.
[24] Silvestri, L.; Bassani, F.; Czajkowski, G.; Davondi, B. *Eur. Phys. J. B* **2002,** *27,* 89–102.
[25] Dynes, J.F.; Frogley, M.D.; Rodger, J.; Phillips, C.C. *Phys. Rev. B* **2005,** *72,* 085323-1–7; Dynes, J.F.; Paspalakis, E. *Phys. Rev. B* **2006,** *73,* 233305-1–4.
[26] Dynes, J.F.; Frogley, M.D.; Beck, M.; Faist, J.; Phillips, C.C. *Phys. Rev. Lett.* **2005,** *94,* 157403-1–4.
[27] Wu, J.H.; Gao, J.Y.; Xu, J.H.; Silvestri, L.; Artoni, M.; La Rocca, G.C.; Bassani, F. *Phys. Rev. Lett.* **2005,** *95,* 057401-1–4; Wu, J.H.; Gao, J.Y.; Xu, J.H.; Silvestri, L.; Artoni, M.; La Rocca, G.C.; Bassani, F. *Phys. Rev. A* **2006,** *73,* 053818-1–6.
[28] Ku, P.C.; Sedgwick, F.; Chang-Hasnain, C.J.; Palinginis, P.; Li, T.; Wang, H.; Chang, S.W.; Chuang, S.L. *Opt. Lett.* **2004,** *29,* 2291–2294; Sarkar, S.; Guo, Y.; Wang, H. *Opt. Express* **2006,** *14,* 2845–2850; Yelin, S.F.; Hemmer, P.R. *Phys. Rev. A* **2002,** *66,* 013803-1–5.
[29] Joshi, A.; Xiao, M. *Appl. Phys. B: Lasers Opt.* **2004,** *79,* 65–69; Li, J.H.; Yang, X.X. *Eur. Phys. J. B* **2006,** *53,* 449–454.
[30] Ning, C.Z. *Phys. Rev. Lett.* **2004,** *93,* 187403-1–4; Liu, A.; Ning, C.Z. *Appl. Phys. Lett.* **1999,** *75,* 1207–1209.
[31] Talanina, I. *J. Opt. Soc. Am. B* **1996,** *13,* 1308–1313; *Phys. Lett. A* **1998,** *241,* 179–185; Talanina, I.; Burak, D.; Binder, R.; Giessen, H.; Peyghambarian, N. *Phys. Rev. E* **1998,** *58,* 1074–1080; Biancalana, F.; Healy, S.; Fehse, R.; O'Reilly, E. *Phys. Rev. A* **2006,** *73,* 063826-1–13.
[32] Paspalakis, E.; Kanaki, A.; Terzis, A.F. *Proc. SPIE* **2007,** *6582,* 65821N-1–9; Li, J. *Phys. Stat. Sol. (b)* **2007,** *244,* 3333–3339; Hao, X.; Li, J.; Liu, J.; Song, P.; Yang, X. *Phys. Lett. A* **2008,** *372,* 2509–2513.
[33] Yang, W.X.; Hou, J.M.; Lee, R.K. *Phys. Rev. A* **2008,** *77,* 033838-1–7.
[34] Sun, H.; Gong, S.; Nill, Y.; Jin, S.; Li, R.; Xu, Z. *Phys. Rev. B* **2006,** *74,* 155314-1–5.
[35] Paspalakis, E.; Simserides, C.; Baskoutas, S.; Terzis, A.F. *Phys. E* **2008,** *40,* 1301–1304; Paspalakis, E.; Tsaousidou, M.; Terzis, A.F. *J. Appl. Phys.* **2006,** *100,* 044312-1–8; *Phys. Rev. B* **2006,** *73,* 125344-1–5.
[36] Semtsiv, M.P.; Ziegler, M.; Masselink, W.T.; Georgiev, N.; Dekorsy, T.; Helm, M. *J. Appl. Phys.* **2005,** *97,* 113538-1–8.
[37] Harris, S.E. *Phys. Rev. Lett.* **1989,** *62,* 1033–1036.